Surface Modification of Nano-Fe_3O_4 with EDTA and Its Use in H_2O_2 Activation for Removing Organic Pollutants

Mingqiong Wang,[a] Nan Wang,[a] Heqing Tang,*[, b] Meijuan Cao,[c] Yuanbin She[c] and Lihua Zhu*[, a]

[a] *College of Chemistry and Chemical Engineering, Huazhong University of Science and Technology, Wuhan 430074, P.R. China. Fax: +86 27 87543632; Tel: +86 27 87543432; E-mail: lhzhu63@yahoo.com.cn (L. Zhu)*

[b] *Hubei Key Laboratory for Catalysis and Material Science, College of Chemistry and Material Science, South-Central University for Nationalities, Wuhan 430074, P. R. China.*

E-mail:hqtang62@yahoo.com.cn (H. Tang)

[c] *College of Environmental and Energy Engineering, Beijing University of Technology, Beijing 100124, P.R. China*

Contents:

S1. (a) Analytical methods of PCP, SMM, and EDTA with HPLC.

The concentrations of PCP, SMM and EDTA were monitored by high-performance liquid chromatography on a PU-2089 HPLC (JASCO, Japan), equipped with a C18ODS column and an UV detector. PCP was determined at 218 nm with a mobile phase of methanol: water (80:20, v/v) at pH 3.4 (adjusted with phosphate); SMM was analyzed at 265 nm with a mobile phase of methanol: water (35:65, v/v). EDTA was detected as Fe^{3+}-EDTA complex at 258 nm with a mobile phase of formate buffer (100%) within 2 mmol L^{-1} TBA-Br. Prior to analysis, 100 μL EDTA samples and 100 μL Fe^{3+} solution were mixed with 1 mL of formate buffer solution which offered the optimal pH for the complex of EDTA with Fe^{3+}. The flow rate and injection volume were 1.0 mL min^{-1} and 20 μL through all the experiments, respectively. The formate buffer at pH 3.3 consisted of 5 mmol L^{-1} sodium formate and 15 mmol L^{-1} formic acid. The Fe^{3+} solution was prepared by dissolving 10 mmol L^{-1} $Fe(NO_3)_3 \cdot 9H_2O$ in a solution of 10 mmol L^{-1} HNO_3.

(b) Sorption experiment of fluoride

500 μL of fluoride solution (0.1 mol L^{-1}, 5.0×10^{-5} mol) was added into 50 mL Fe_3O_4 MNPs solution (1.2 mmol L^{-1}, 0.014 g) at pH 5.0, followed by shaking on a constant-temperature shaker (SHZ-82A, Guohuayiqi, China) at 150 rpm at 40 ºC for 2h in

order to reach equilibrium. At the end of the experiment, the adsorbent particles were separated out from the suspensions by using a magnet, and then the suspensions were filtered through a 0.22 μm pore size filter to remove any retained solid particles before analysis of the fluoride concentration.

Fluoride concentration of the above supernatant solution was analyzed by fluoride ion selective electrode after adding 10 mL the total ionic strength adjustment buffer (TISAB), which was prepared by dissolving of $NaNO_3$ (85 g) and sodium citrate ($C_6H_5Na_3O_7 \cdot 2H_2O$, 58.8g) in distilled water (about 800 mL), while stirring the solution, adjusting the pH to 5.0 - 5.5 with 3 mol HCl and finally diluting to 1 L with water in a 1 L volumetric flask. The equilibrium concentration of fluoride was 8.8×10^{-4} mol L^{-1} (50 mL, 4.4×10^{-5} mol). The total site density (T_{sd}, site number per gram of catalyst) and site density (S_d, site number per unit of surface area) was calculated using the following formula: $T_{sd} = (n_0 - n_e)/W$, $S_d = T_{sd}/S$, where n_0 and n_e are the initial and equilibrium amount of fluoride in our studied system(5.0×10^{-5}, 4.4×10^{-5} mol), respectively, W and S are the mass and specific surface area of the Fe_3O_4 MNPs used in the experiment (0.014 g, 82.5 $m^2 g^{-1}$), respectively.

S2. Methods and model of the density functional theory (DFT) calculations

The adsorption geometry and electronic structure of H_2O_2 or EDTA on Fe_3O_4(111) surface were successfully simulated according to Density Functional Theory (DFT). All calculations were carried out by using Dmol^3 package in the Material Studio 4.4 software[S1-S2]. The configuration optimization was implemented by Vosko-Wilk-Nusair (VWN) functional of local density approximation (LDA) method with the double numerical basis sets plus polarization function (DNP).[S2] The core of Fe atoms were treated with effective core potentials (ECP), and the one of other atoms

(containing O, H, C and N) were treated with all electrons. Brillouin-zoneintegration of the Monkhorst-Pack grid parameter was set to Medium, and the Methfessel-Paxton smearing of 0.005 Ha was utilized. To achieve the structure optimization and energy calculation, the convergence criteria of the energy tolerance, the displacement tolerance and the maximum force tolerance were set to 2×10^{-5} a.u., 5×10^{-4} nm and 4×10^{-3} Ry/a.u., respectively. The remaining parameters are the default values. Without counting the adsorbate, the vacuum between the slabs was set to span a range of 11 Å to exclude the interaction between the slabs.[S3]

Fe_3O_4 possesses a cubic inverse spinel structure with lattice constant of 0.8396 nm, being composed of eight tetrahedral sites occupied by Fe^{3+} and 16 octahedral sites equally shared by Fe^{3+} and Fe^{2+}. [S4] As one of the predominant natural growth faces, Fe_3O_4(111) shows the higher catalytic activity than the other surfaces.[S5] Moreover, Fe_{tet1}-terminaion and Fe_{oct2}-terminaion are the two most stable terminations of Fe_3O_4(111) surface, [S6] thus, the adsorption of H_2O_2 molecular in our study was performed on these two terminations. In addition, we mainly considered the high-symmetry adsorption sites including four vacancies (hollow), the double bridge site (bridge) and a heavy top site (top).

For bare Fe_3O_4, H_2O_2 prefers to adsorb on the Fe_3O_4 (111) surface through hollow sites rather than via top and bridge modes (Fig. S1b). In the optimal adsorption configuration of hollow mode, the O atoms of H_2O_2 directly interact with the four coordinate iron ion, which shortens the O-O bond of H_2O_2 from 1.464 to 1.300 Å. In the presence of both EDTA and H_2O_2, EDTA is adsorbed on the Fe_3O_4 surface to form the monodentate outer-sphere complexes, while H_2O_2 is hydrogen bonded to O atom on the top sites of Fe_3O_4 through one H atom of the former. However, the hydrogen bonding between the other H atom of H_2O_2 and the N atom and COO^- of

EDTA made the H_2O_2 adsorption configuration changes to a more stable bridge mode (Fig. S1c). At the final state of the H_2O_2 adsorption, the O-O bond of H_2O_2 is stretched up to 1.380 Å in the presence of EDTA relative to that (1.300 Å) in the absence of EDTA. The calculated value of the H_2O_2 adsorption energy (E_{ads}) in the EDTA-H_2O_2-Fe_3O_4 system is –2452 kJ/mol, which is more negative than that (–87 kJ/mol) in the H_2O_2-Fe_3O_4 system. It is known that the more negative the E_{ads} is, the more stable the adsorption mode is.[S7] This suggests that the presence of EDTA is beneficial for the adsorption of H_2O_2 on the Fe_3O_4(111) surface.

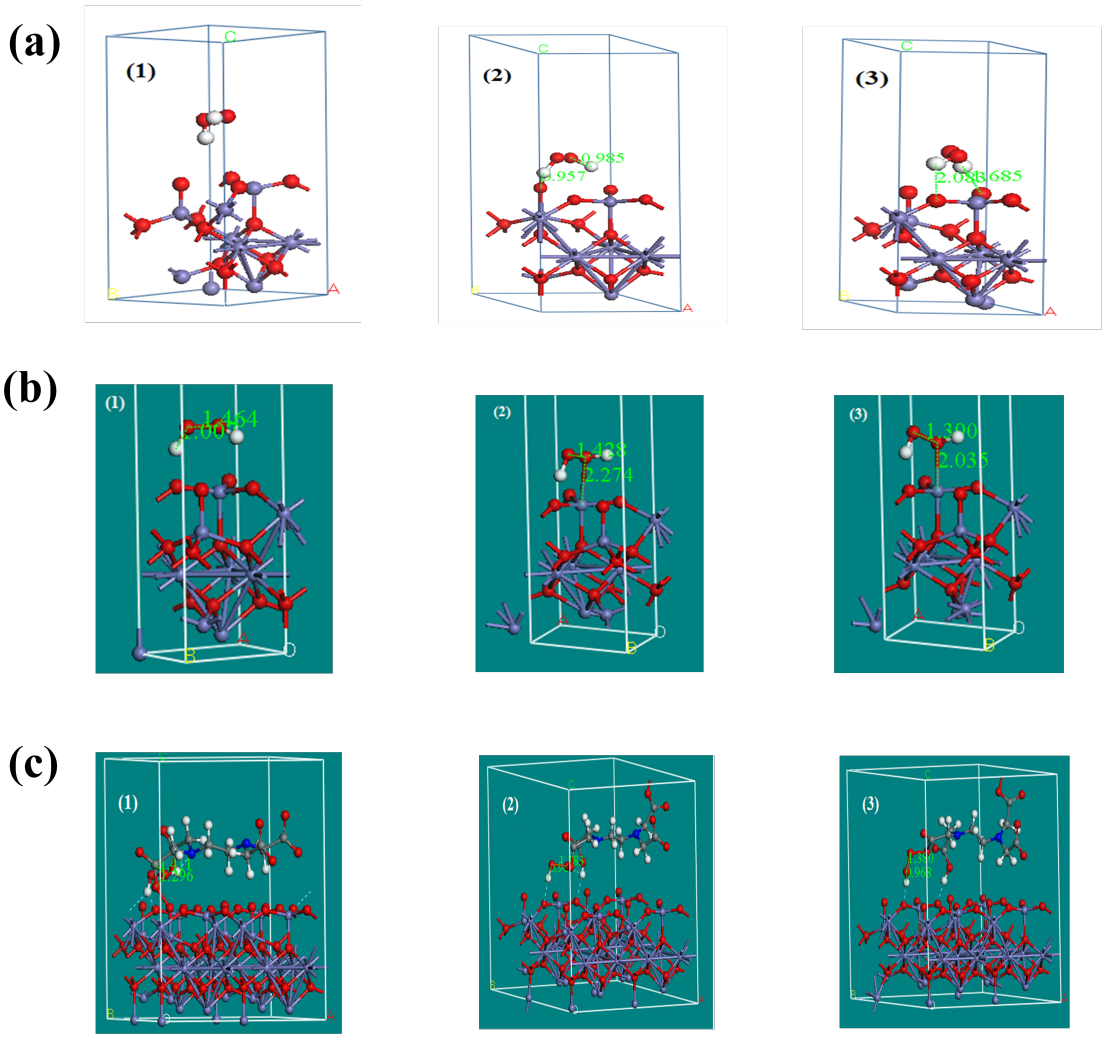

Fig. S1. (a) Three possible modes of H_2O_2 adsorption on the $Fe_3O_4(111)$ surface: (1) hollow, (2) top, and (3) bridge. (b, c) H_2O_2 adsorption states on the $Fe_3O_4(111)$ surface in the absence (b) and presence of EDTA (c): (1) initial state, (2) intermediate state and (3) final state of adsorption. The violet, red, grey, white and blue spheres stand for Fe, O, C, H and N atoms.

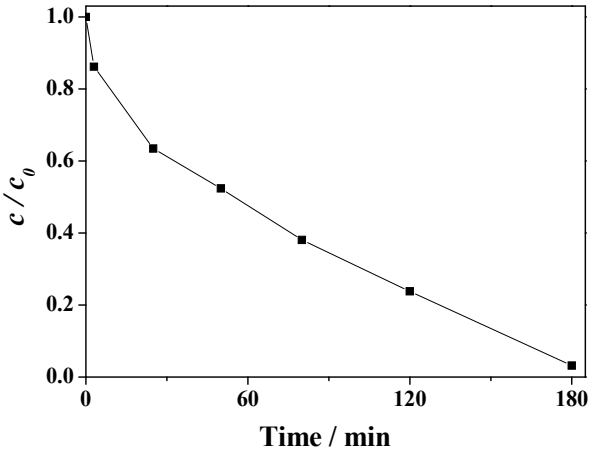

Fig. S2. Degradation of EDTA (0.5 mmol L^{-1}) in the Fe_3O_4 suspensions (1.2 mmol L^{-1}) containing RhB (0.02 mmol L^{-1}) and H_2O_2 (5 mmol L^{-1}) at pH 5.0 and 40 °C.

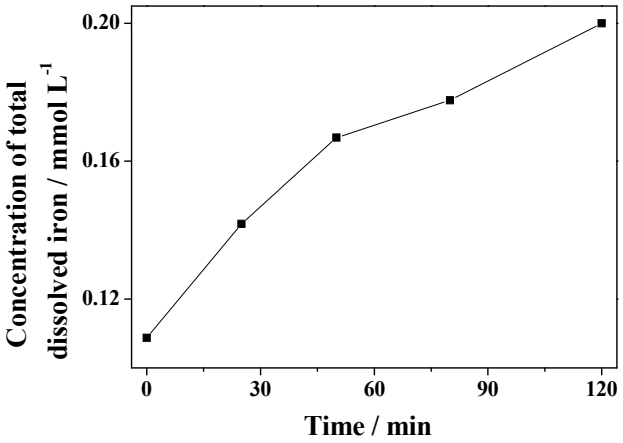

Fig. S3. Concentration of total dissolved iron in the Fe_3O_4 suspensions (1.2 mmol L^{-1}) containing EDTA (0.5 mmol L^{-1}), H_2O_2 (5 mmol L^{-1}) and RhB (0.02 mmol L^{-1}) at pH 5.0 and 40 °C.

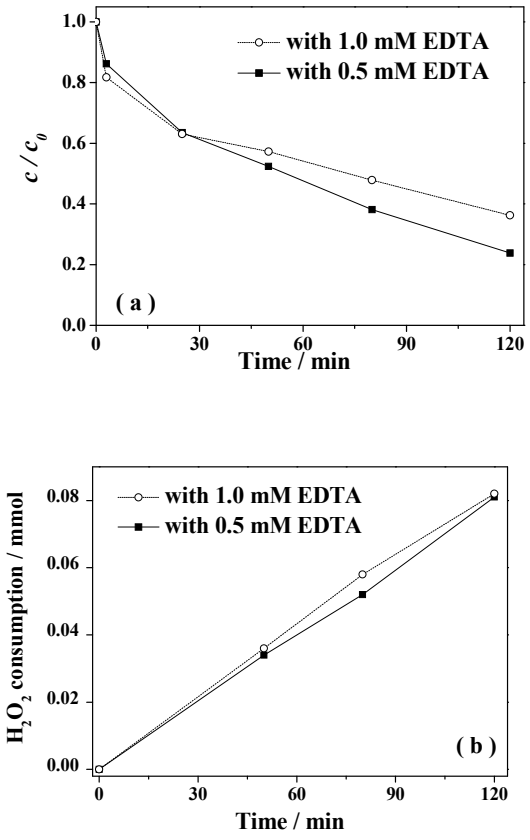

Fig. S4. (a) Degradation of EDTA and (b) H_2O_2 consumption in the Fe_3O_4 suspensions (1.2 mmol L^{-1}) containing RhB (0.02 mmol L^{-1}), H_2O_2 (5 mmol L^{-1}), and EDTA at pH 5.0 and 40 °C.

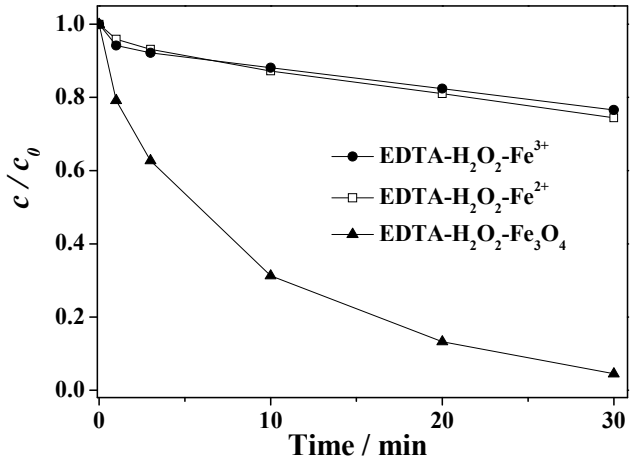

Fig. S5. Degradation of RhB in different systems at 60 °C. Reaction conditions: pH 5.0, RhB 0.02 mmol L^{-1}, 0.5 mmol L^{-1} EDTA, 5 mmol L^{-1} H_2O_2, 0.29 mmol L^{-1} Fe^{2+} or Fe^{3+}, 1.2 mmol L^{-1} Fe_3O_4, if not specified.

S3. Enhanced Fe^{3+}/Fe^{2+} recycle on the surface of EDTA-modified Fe_3O_4

To verify the promotion of the Fe^{3+}/Fe^{2+} recycle by EDTA, the chemical composition on the Fe_3O_4 surface after catalytic reactions were measured by Raman technology. In the Raman spectrum of the bare Fe_3O_4 (curve 1 in Fig. S6), a series of characteristic peaks appeared at 350 cm^{-1}(E_g), 500 cm^{-1}(T_{2g}), 697 cm^{-1} (A_{1g}) and 1384 cm^{-1} ($2\nu_{as(Fe\text{-}O\text{-}Fe)}$), which are assigned to Fe-O symmetrical bending, Fe-O-Fe symmetrical stretching, Fe-O-Fe asymmetrical stretching, and 2 times of Fe-O-Fe asymmetrical stretching, respectively, being consistent with the data reported on the literature.[S8-S10] After Fe_3O_4 was exposed to H_2O_2 solution for 2 h, the characteristic peaks of Fe_3O_4 at 350, 500, and 1384 cm^{-1} were shifted and/or broadened, and several new peaks

appeared at 215, 280, and 399 cm^{-1} (curve 3 in Fig. S6). Compared with the reference compound Fe_2O_3 (curve 4 in Fig. S6), which exhibited absorption of A_{1g} at 215 and 490 cm^{-1}, E_g at 280, 399 and 600 cm^{-1} and $2\nu_{as(Fe\text{-}O\text{-}Fe)}$ at 1303 cm^{-1},[S8,S10] the above-mentioned differences in Raman spectra of Fe_3O_4 in the absence and presence of H_2O_2 indicate that the surface Fe^{2+} dominant over Fe^{3+} to react with H_2O_2, resulting in that the Fe_3O_4 surface is converted to the Fe_2O_3 structure in a certain extent. Because the re-reduction of Fe^{3+} to Fe^{2+} is rather difficult, the slow conversion of Fe^{3+} to Fe^{2+} may gradually lead to the inactivation of the Fe_3O_4 surface for the activation of H_2O_2. If EDTA was present in the H_2O_2-Fe_3O_4 system, it was also found the new peaks at 215 and 280 cm^{-1}, but the characteristic peaks of Fe_3O_4 at 500 and 1384 cm^{-1} were slightly unchanged (curve 2 in Fig. S6), implying the surface of Fe_3O_4 catalyst could keep its own features within EDTA much better than that without EDTA. On the other word, the present EDTA can promote the Fe^{3+}/Fe^{2+} recycling on the Fe_3O_4 surface during the activation of H_2O_2.

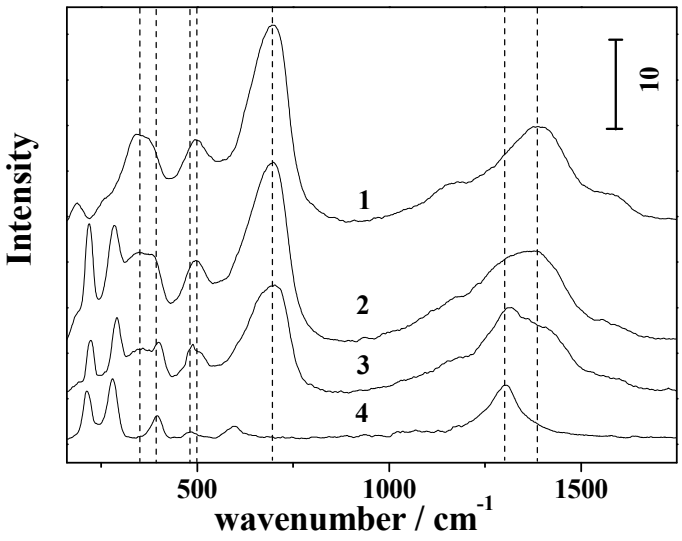

Fig. S6. Raman spectra of (1) bare Fe_3O_4, (2) H_2O_2-EDTA-Fe_3O_4, (3) H_2O_2-Fe_3O_4 and (4) Fe_2O_3. H_2O_2-EDTA-Fe_3O_4 and H_2O_2-Fe_3O_4 represented Fe_3O_4 MNPs

being reacted with H_2O_2 for 2 h at pH 5.0 and 40 °C in the presence and absence of EDTA, respectively.

SCHEME S1.Three modes of coordination between EDTA and metal (Fe).

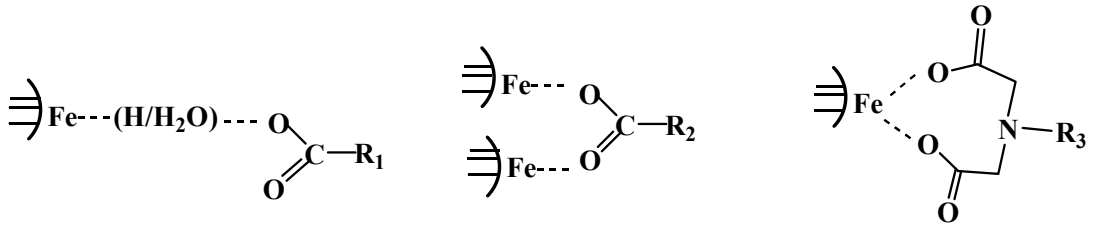

(a) Monodentate binding **(b) Bridging bidentate** **(c) Chelating binding**

S4. References

(S1) A. K. Kandalam, B. Chatteriee, S. N. Khanna, B. K. Rao, P. Jena and B. V. Reddy, *Surf. Sci.*, 2007 **601**, 4873-4880.

(S2) H. Munakata, Y. Oumi and A. Miyamoto, *J. Phys. Chem. B*, 2001, **105**, 3493-3501.

(S3) W. K. Chen, M. J. Cao, S. H. Liu, C. H. Lu, Y. Xu and J. Q. Li, *Chem. Phys. Lett.*, 2006, **417**, 414-418.

(S4) S. Soeya, J. Hayakawa, H. Takahashi, K. Ito, C. Yamamoto, A. Kida, H. Asano and M. Matsui, *Appl. Phys. Lett.*, 2002, **80**, 823-825.

(S5) N. D. Spencer, R. C. Schoonmaker and G. A. Somorjai, *J. Catal.*, 1982, **74**, 129-135.

(S6) T. Yang, X. D. Wen, C. F. Huo, Y. W. Li, J. G. Wang and H. J. Jiao, *J. Phys. Chem. C*, 2008, **112**, 6372-6379.

(S7) D. B. Cao, F. Q. Zhang, Y. W. Li and H. J. Jiao. *J. Phys. Chem. B*, 2004, **108**,

9094-9104.

(S8) D. L. A. De Faria, S. Venancio Silva and M. T. De Oliveira, *J. Raman Spectrosc.*, 1997, **28**, 873-878.

(S9) J. D. Cohen, S. Payne, K. S. Hagen and J. Sanders-Loehr, *J. Am. Chem. Soc.*, 1997, **119**, 2960-2961.

(S10) M. Basu, A. K. Sinha, S. Sarkar, M. Pradhan, S. M. Yusuf, Y. Negishi and T. Pal, *Langmuir*, 2010, **26**, 5836-5842.